

Oral delivery of spray dried PLGA/amifostine nanoparticles

Sarala Pamujula, Richard A. Graves, Thomas Freeman, Venkataraman Srinivasan, Levon A. Bostanian, Vimal Kishore and Tarun K. Mandal

Abstract

Amifostine (Ethyol, WR-2721) is a cytoprotective drug approved by the US Food & Drug Administration for intravenous administration in cancer patients receiving radiation therapy and certain forms of chemotherapy. The primary objective of this project was to develop orally active amifostine nanoparticles using spray drying technique. Two different nanoparticle formulations (Amifostine-PLGA (0.4:1.0 and 1.0:1.0)) were prepared using a Buchi B191 Mini Spray Dryer. A water-in-oil emulsion of amifostine and PLGA (RG 502) was spray dried using an airflow of 600 L h⁻¹ and input temperature of 55°C. A tissue distribution study in mice was conducted following oral administration of the formulation containing drug-polymer (0.4:1.0). The efficiency of encapsulation was 90% and 100%, respectively, for the two formulations while the median particle sizes were 257 and 240 nm, with 90% confidence between 182 and 417 nm. Since amifostine is metabolized to its active form, WR-1065, by intracellular alkaline phosphatase, the tissue levels of WR-1065 were measured, instead of WR-2721. WR-1065 was detected in significant amounts in all tissues, including bone marrow, jejunum and the kidneys, and there was some degree of selectivity in its distribution in various tissues. This work demonstrates the feasibility of developing an orally effective formulation of amifostine that can be used clinically.

Introduction

Amifostine, also known in the literature as Ethiofos, Ethyol (MedImmune, USA) or WR-2721, an organic thiophosphate prodrug, is dephosphorylated by alkaline phosphatase in tissue to the active free thiol metabolite (WR-1065). The drug has been extensively studied both as a cytoprotective and a radioprotective agent. A major limitation of this drug however is that it is not orally active (Bonner & Shaw 2002) and must therefore be administered systemically to be effective. Amifostine is also rapidly cleared from the body and has a short distribution half-life of 0.9 min when administered as a bolus dose or as a 15-min intravenous infusion (Bonner & Shaw 2002; Cassatt et al 2002; Schuchter et al 2002). In an attempt to find an alternative route of administration, several investigators have found that, when compared to intravenous administration, subcutaneous administration provided a more effective dosing regimen, both in terms of a reasonable AUC and decreased toxicity (Godette 2001; Anne & Curran 2002; Bonner & Shaw 2002; Koukourakis et al 2002). Attempts have also been made to develop various formulations of amifostine, such as transdermal patches (Lamperti et al 1990), subcutaneous implants (Srinivasan 2002), pulmonary inhalers and oral sustained-release microspheres (Fatome et al 1987). For example, when co-administered with dimethyl sulfoxide (DMSO) as a transdermal patch, the absorption of amifostine was significantly enhanced (Lamperti et al 1990). Additionally, oral administration of ethyl cellulose microcapsules containing amifostine was also shown to provide radiation protection along with decreased toxicity in mice (Fatome et al 1987). Despite these efforts though, a non-injectable formulation of amifostine for clinical use is still not available.

Since the oral route of drug administration is the most convenient and popular, our goal was to develop an orally active biodegradable sustained-release formulation of amifostine using poly (lactide-co-glycolide) (PLGA) as carrier particles. This goal was

College of Pharmacy,
Xavier University of Louisiana,
New Orleans, LA 70125-1098,
USA

Sarala Pamujula, Richard A.
Graves, Thomas Freeman, Levon
A. Bostanian, Vimal Kishore,
Tarun K. Mandal

Armed Forces Radiobiology
Research Institute, Bethesda,
MD 20889, USA

V. Srinivasan

Acknowledgment and funding:

This work was funded in part by the NIH/NIGMS grants nos GM08008-32 and GM08008-32S1. The authors thank Dr Yushu Gao at the Xavier University College of Pharmacy for his technical help in Zeta potential measurements.

Correspondence: T. K. Mandal,
College of Pharmacy,
Xavier University of Louisiana,
1 Drexel Dr., New Orleans,
LA 70125-1098, USA.
E-mail: tmandal@xula.edu

justified based upon earlier work. A number of investigators had already shown that certain polymers could be used to carry drug particles across the intestinal mucosa (Florence 1997; Hussain et al 2001). For example, using calves, uptake of small resin particles (1–5 μm) following oral administration was demonstrated by the accumulation of these particles in the tonsils, small intestine and certain lymph nodes (Payne et al 1960). Sanders & Ashworth (1961) were able to detect a large number of intact particles in the jejunal epithelial cells of rats following oral administration of a concentrated emulsion of polystyrene latex. Particles of 100–200 nm diameter were occasionally observed between the microvilli or in the terminal web and the intracellular spaces of the epithelium, and many more were found in the cytoplasm of the jejunal epithelial cells where they were always enclosed in vesicles. Jani et al (1990) reported at least 30% absorption of 50-nm polystyrene particles following oral administration to male rats. Histological studies showed that 6–7% of these particles accumulated in the liver, spleen, blood, bone marrow and kidneys. Particles of 100 nm to 1 μm were found in the serosal layer of the Peyer's patches. However, larger particles (3 μm) were found to be absorbed and immobile within the submucosal layers of the stomach and also of the Peyer's patches. Eldridge et al (1990) and LeFevre et al (1978, 1980) also published similar findings, with particles of 6 μm in diameter. Jenkins and co-workers (Jenkins et al 1994) have reported the size dependence of uptake over the range of 150–1000 nm. There are now several reports in the literature on the size dependence of nanoparticles absorption (Alpar et al 1989; Jani et al 1989, 1992; Ebel 1990; Bockmann et al 2000; Powel et al 2000; De Jaeghere et al 2000). In particulate drug delivery, both the rate and extent of uptake and translocation are key factors. Eldridge's data (Eldridge et al 1990) suggest that the process is relatively rapid with microparticles appearing in the mesentery lymph and beginning to accumulate 2 h after a single oral dose. Recent studies on PLGA particles from 100 nm to 10 μm showed that the former diffused throughout the submucosal layers while the latter were predominantly localized in the epithelial lining of the tissue (Guterres et al 1995; Desai et al 1996). It seems that particles in the range 3–10 μm are sequestered within the Peyer's patches and do not migrate into the mesenteric lymph nodes (Florence & Jani 1993).

In our previous work with amifostine (Pamujula et al 2004), we demonstrated that the drug was compatible with PLGA and that the microcapsules prepared by solvent evaporation technique showed sustained amifostine release up to 96 h. These early formulations suffered from two main disadvantages. Not only was amifostine incorporation low (37% or less at 5% loading), but also the average particle size of the microcapsules was larger than 50 μm . Since the biologically effective dose for amifostine is very high, we projected that the final formulation needed to contain at least 20% amifostine, and that the average particle size needed to be less than 10 μm , to allow for successful absorption through Peyer's patches. To achieve these goals, we abandoned the solvent evaporation technique in favour of spray drying. The

spray drying technique consists of converting drug–polymer solution or suspension in a suitable solvent into fine particles by spraying through an atomization nozzle into hot air. The solvent within the atomized droplets evaporates very quickly and solid nanoparticles and microparticles are formed. Mu & Feng (2001) have used this technique to prepare paclitaxel-loaded PLGA nanoparticles. This technique has also been used by Wang & Wang (2003) to encapsulate etanidazole. This report now presents the results obtained from our spray dried PLGA/amifostine nanoparticles.

Materials and Methods

Materials

The copolymer poly (DL-lactic–glycolic acid), PLGA 50:50 (RG 502; inherent viscosity 0.2 dL g⁻¹) was obtained from Boehringer Ingelheim (Germany). The surfactant, L- α phosphatidylcholine was obtained from Avanti Polar-Lipids, Inc. (Birmingham, AL). Amifostine, chloroform and dichloromethane were obtained from Sigma Chemical Co. (St Louis, MO).

Preparation of spray dried nanoparticles

Two different nanoparticle formulations (amifostine–PLGA (0.4:1.0 and 1.0:1.0), described as formulation A and B, respectively) were prepared using a Buchi B191 Mini Spray Dryer (Switzerland), with a standard 0.7-mm nozzle. The inlet air temperature, aspirator, liquid flow and compressed spray air flow were set at 55°C, 70%, 3.5 mL min⁻¹ and 600 L h⁻¹, respectively. A specific amount of amifostine (400 mg formulation A, 1000 mg formulation B) was dissolved in a specific volume (1 mL for formulation A, 2 mL for formulation B) of de-ionized water and the solution was emulsified in 50 mL of dichloromethane containing 1 g of PLGA, RG 502 (Table 1).

Table 1 Physical characteristics of amifostine nanoparticles

	Formulation A	Formulation B
Efficiency of encapsulation (%) (s.e.m.)	90.90 (0.16)	100.03 (2.01)
Median particle size (nm) (90% confidence)	257 (182–417)	240 (182–417)
Morphology	Smooth and spherical	Smooth and spherical
Zeta potential (mV) (s.e.m.)	+2.8 (1.1)	–13.8 (1.1)
Glass transition temperature (T _g , °C) (s.e.m.)	35.5 (0.10)	36.1 (0.86)
Amifostine melting point (°C)	138.1 (4.4)	141.2 (5.5)

Formulation A: 400 mg of amifostine dissolved in 1 mL of de-ionized water; amount of PLGA 1000 mg. Formulation B: 1000 mg of amifostine dissolved in 2 mL of de-ionized water; amount of PLGA 1000 mg. T_g for PLGA (RG 502), 35.11°C. Pure amifostine melting point, 141.0°C.

Ethyl acetate (bp 60°C, flash point 43°C) and dichloromethane (bp 77°C, flash point, -4°C) are two commonly used organic solvents for microencapsulation of drugs (Wang & Wang 2003). Dichloromethane was preferred over ethyl acetate because of the low flash point and high boiling point of the latter. The polymer solution was previously mixed with 1.25 mL of lipophilic surfactant L- α -phosphatidylcholine in chloroform (8 mg mL⁻¹). L- α -Phosphatidylcholine has been used extensively to stabilize water-in-oil emulsions (Feng & Huang 2001). It has several advantages over other lipophilic surfactants (e.g., it is soluble in many organic solvents, including dichloromethane, which is a common solvent used for PLGA microcapsules). The emulsification was carried out by sonication at output 4 (50 W) for 30 s (ultrasonic probe; Sonic & Materials Inc., Danbury, CT). When the resultant emulsion was fed to the nozzle with a peristaltic pump, atomization occurred by the force of the compressed air, disrupting emulsion into small droplets. The droplets, together with hot air, were blown into a chamber where the dichloromethane was evaporated and discharged through an exhaust tube. The fine nanoparticles accumulated into the glass collection chamber were collected and freeze-dried (-20°C; 10 × 10⁻⁴ mbar; FreeZone 6, Labconco Corporation, Kansas City, MO) for 24 h for complete removal of any residual solvent. The processing conditions used for the preparation of blank nanoparticles were exactly the same as the drug loaded formulations, except 1 mL of de-ionized water rather than amifostine aqueous solution was emulsified in dichloromethane.

HPLC Analysis

The analysis of amifostine was performed using a rapid and sensitive HPLC method (Srinivasan et al 2002). The chromatographic system consisted of a Waters Model 600 programmable solvent delivery module, Waters Model 717plus auto sampler (Waters, Milford, MA) and a BAS LC-44 Model MF-9000 electrochemical detector (Bioanalytical Systems, West Lafayette, IN). The chromatography was performed under the following specific conditions: column μ bondpack C-18 (Waters 10 μ m, 3.9 × 300 mm); mobile phase 96 mM monochloroacetic acid pH 2.8, 3 mM hexane sulfonic acid, 3.5% acetonitrile and 1 μ M 2-mercaptoethylamine. The mobile phase was vigorously purged with helium gas for 15 min before use; flow rate 1 mL min⁻¹. The detector (Hg/Au electrode) oxidation potential was set at +0.2 V and the injection volume was 20 μ L. The concentration of amifostine in each sample was determined by intrapolating the peak height to the amifostine standard curve and each sample was analysed in triplicate.

Efficiency of encapsulation of amifostine

The efficiency of encapsulation was determined in triplicate by measuring the total amount of amifostine present in a given sample. A 20-mg sample was dissolved in 1 mL of dichloromethane and the solution was extracted with 10 mL of 0.15% aqueous Tween 80. The addition of

aqueous Tween 80 precipitated the polymer and allowed for the extraction of amifostine into the aqueous phase. The precipitated polymer was separated by ultracentrifugation for 10 min and the supernatant was analysed for amifostine.

Particle size and morphology

Particle size distribution was determined by a Coulter LS130 analyzer (Beckman Coulter Inc., Fullerton, CA). This technique measures the size of particles dispersed in a medium by the scattering pattern of a traversing laser light. The samples were analysed in de-ionized water and the Fraunhofer method was utilized to calculate the size distribution. The particle size calculations assume the presence of spherical particles and are based on calculated volumes of spheres. For each sample, a background run of de-ionized water was performed. A sample of nanoparticles (2 mg) was added to the de-ionized water in a micro sample cell and counting was performed for 120 s. After subtraction of the background, the particle size distribution calculation was performed. Each experiment was performed in triplicate. Morphology of the nanoparticles was examined by using a variable pressure scanning electron microscopy (SEM) (S-3000N, Hitachi, Tokyo, Japan). Samples for SEM were mounted on metal stubs and coated with gold to a thickness of 200–500 Å.

Thermal characterization

Thermal analysis of the nanoparticles was performed by differential scanning calorimetry (DSC) using a calorimeter (TA 2920) fitted with a refrigeration unit (TA Instruments, New Castle, DE). Drug-loaded nanoparticles and pure PLGA (RG 502) were used for thermal characterization. About 5 mg of a sample was weighed, crimped into an aluminium pan and analysed at a scanning rate of 5°C min⁻¹. The glass transition temperature (T_g) was calculated using TA universal analysis software by extrapolating the linear portion of the thermograms above and below the glass transition point and determining the midpoint.

Attenuated total reflectance (ATR) infra-red spectroscopic analysis

Infrared spectra of amifostine, PLGA, blank nanoparticles and amifostine-loaded nanoparticles were obtained using a PerkinElmer Spectrum One spectrometer (PerkinElmer, Boston, MA). A universal attenuated total reflectance (UATR) accessory was used and the spectra were collected with no further processing of the samples.

Zeta potential

The zeta potential of nanoparticles was measured using a Malvern Zetasizer 2000 (Malvern Instruments, Malvern, UK). The experiments were performed in de-ionized and

de-aerated water, and all measurements were performed in triplicate.

Tissue distribution study

Animals and dosing

Animals were cared for in compliance with protocols approved by the Xavier University of Louisiana Committee on Animal Care, and in conformity with the Principles of Laboratory Animal Care (NIH publication no. 85-23, revised 1985). Male CD2F1 mice, 25–27 g and 8–10 weeks old, housed 5 per cage in air-conditioned facility ($21 \pm 1^\circ\text{C}$; $50 \pm 10\%$ relative humidity) had free access to standard mouse chow and water. The nanoparticles suspended in 0.15% Tween 80 were administered by oral gavage at a dose equivalent to 250 mg kg^{-1} amifostine. Mice were sacrificed at various times after oral feeding and each time group consisted of three mice. Blood samples ($300 \mu\text{L}$ each) collected from the heart were precipitated within 1 min after collection with an equal volume of ice-cold perchloric acid–EDTA (0.5 M/0.16 M). The precipitates were centrifuged at $10\,000 \text{ rev min}^{-1}$ at 4°C for 10 min and supernatants were stored at -70°C until the day of analysis. All other tissue samples were stored unprocessed at -70°C until analysis. In addition, the femurs were also collected and dropped immediately into liquid nitrogen followed by transfer to -70°C until the day of analysis. All analysis was completed within 72 h after collection and the stability of amifostine during this period at -70°C was confirmed.

Analysis of tissue samples

On the day of analysis, the frozen tissues were homogenized in water (20% w/v), precipitated with an equal volume of perchloric acid–EDTA and centrifuged at $10\,000 \text{ rev min}^{-1}$ for 10 min at 4°C . The supernatants were analysed for WR-1065 as described below. The bone marrow was first flushed with 1 mL water and the mixture was prepared for analysis as done for the tissues.

Since amifostine (WR-2721) is a prodrug and is metabolized to its active form WR-1065 by intracellular alkaline phosphatase, the tissue levels of WR-1065, instead of amifostine, were measured. With the exception of the mobile phase, WR-1065 analysis was done using the HPLC method described earlier for amifostine. The mobile phase for WR-1065 consisted of 100 mM monochloroacetic acid, pH 2.8, 1.5 mM hexane sulfonic acid, 9% acetonitrile and $0.5 \mu\text{M}$ 2-mercaptoethylamine.

Statistical analysis

The efficiency of encapsulation of amifostine, median particle size, zeta potential and T_g were compared by a non-parametric test, Mann-Whitney *U*-test using SAS software package. A *P* value of < 0.05 was considered as evidence of a significant difference. All experiments were conducted in triplicate and the data presented are the mean \pm standard error (s.e.).

Results and Discussion

Efficiency of encapsulation

The efficiency of encapsulation of amifostine was determined by measuring the total amount of amifostine present in each 20-mg sample (i.e. core loading experimental), and comparing this value with the expected amount of amifostine in each of the samples based on the drug loading during the preparation (i.e. core loading theoretical). The effect of drug loading was evaluated by preparing two groups of nanoparticles using 29% and 50% w/w amifostine (Table 1). Both formulations contained the same amount of PLGA (1000 mg). The efficiency of encapsulation of formulation A was approximately 91% and that of formulation B was 100%. Thus, while formulation A showed a small amount of drug loss, the formulation B showed no such loss. Other than the quantity of amifostine used, the only other difference between the methods used for these two formulations was the volume of water initially used to dissolve the drug. Formulation A was prepared with 1 mL of water and it was difficult to quantitatively transfer the entire amifostine solution to the PLGA solution; it is this small initial loss that may have reduced the final drug content of this formulation.

Thermal characterization

The DSC traces obtained from the analysis of the amifostine-loaded nanoparticles (formulations A and B) showed no significant difference ($P > 0.05$) in the position of the glass transition temperature (T_g) of PLGA. However, both of the formulations showed about 5°C increase in the position of the T_g of PLGA compared with the blank nanoparticles (Figure 1; only one DSC thermogram of drug loaded nanoparticles, formulation A, was included for the clarity of the figure). There was no significant difference in the position of the melting peak of amifostine in the nanoparticles when compared with amifostine

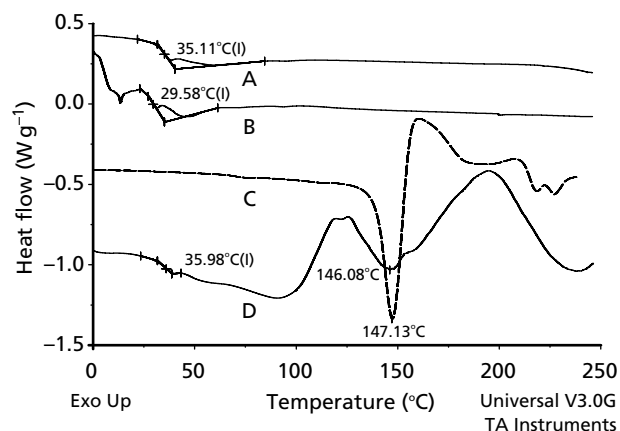


Figure 1 DSC thermograms of PLGA (A), blank nanoparticles (B), amifostine (C) and amifostine-loaded nanoparticles, formulation A (D).

alone, although a wider melting endotherm was observed. When a drug is mixed with a polymer during the preparation of nanoparticles, there are generally three probabilities: the drug and polymer form a solid solution, in which case there is a shift in the position of the T_g of the polymer due to the plasticizing/anti-plasticizing effect of the drug, and the endotherm for the melting of the drug is absent in the nanoparticles; the drug is dispersed in the polymer in an amorphous form, in which case the T_g of the polymer is not affected and the melting endotherm for the drug is absent in the nanoparticles; or the drug is dispersed in the polymer in a crystalline form, in which case there is no change in the position of the T_g of the polymer or the melting endotherm of the drug. For the amifostine-loaded nanoparticles prepared in this study, it appears that, due to the high drug loading of the nanoparticles, a combination of two processes occurred during nanoparticle preparation. Part of the amifostine formed a solid solution with PLGA, causing an increase in the T_g of PLGA by an anti-plasticizing effect. The remaining portion of the amifostine was present in crystalline form dispersed in the polymer as indicated by the absence of any change in the position of the melting peak of amifostine in the nanoparticles. The broadening of the melting peak of amifostine in the nanoparticles can be attributed to the presence of PLGA, which acts as an impurity.

To further investigate the possible occurrence of chemical changes or interaction of amifostine with PLGA, infrared spectra of amifostine, PLGA, blank nanoparticles and two amifostine-loaded nanoparticles were obtained, and are shown in Figure 2 (since no significant differences were observed between formulations A and B, only one infrared spectra of drug-loaded nanoparticles, formulation A, was included for the clarity of the figure). The bands seen in the spectrum of the amifostine-loaded microcapsules appeared to be a combination of the bands of amifostine and PLGA alone (Table 2). There were no changes in the bands corresponding to the functional groups of amifostine or PLGA after microencapsulation,

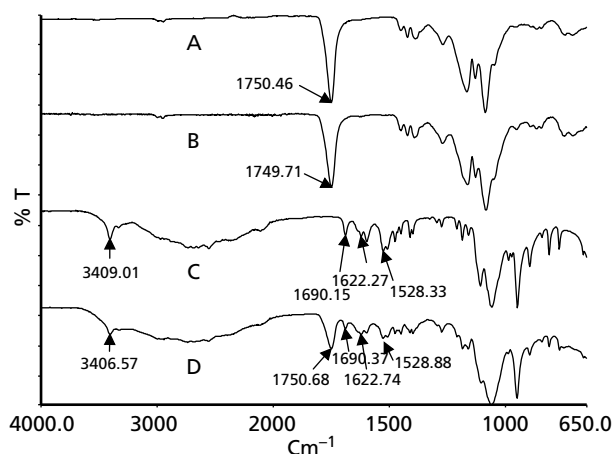


Figure 2 FT-IR spectra of PLGA (A), blank nanoparticles (B), amifostine (C) and amifostine-loaded nanoparticles, formulation A (D).

Table 2 Major bands of FT-IR spectra of PLGA, blank nanoparticles, amifostine and amifostine-loaded nanoparticles, formulation A

Band no.	Wave number (cm^{-1})		Blank nanoparticles	Amifostine-loaded nanoparticles
	Amifostine	PLGA		
1	3409	—	—	3407
2	—	1751	1750	1751
3	1690	—	—	1690
4	1622	—	—	1623
5	1528	—	—	1529

indicating the absence of chemical changes in their structures. Infrared spectroscopy can be used to detect drug-polymer interactions because such interactions usually result in changes in the environment of functional groups, causing changes in the position of the bands that correspond to these functional groups. The absence of any significant shifts in the positions of the absorption bands of amifostine or PLGA indicated that no interaction occurred between amifostine and PLGA during microcapsule formation.

Particle size and morphology

Results of the particle size analysis showed that a change in the drug loading did not significantly affect the median particle size or distribution. The median particle sizes of formulations A and B were 257 and 240 nm respectively, with 90% confidence in the range 182–417 nm (Table 1). Results of the analysis of surface morphology using scanning electron microscopy are shown in Figure 3. The nanoparticles of both formulations A and B were spherical in shape with smooth surfaces. There were no significant morphological differences in these formulations but both formulations contained few collapsed spherical

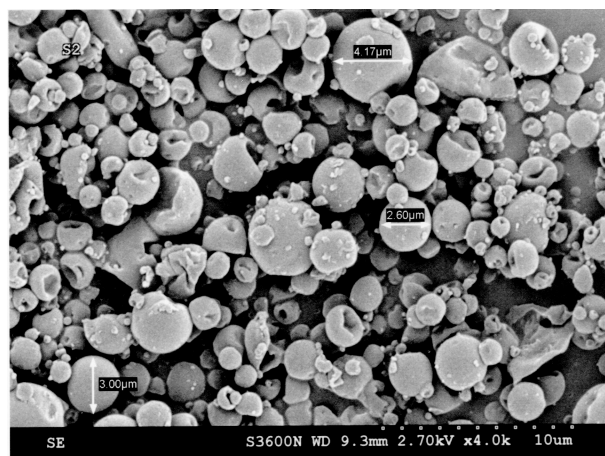


Figure 3 Typical SEM photograph of the nanoparticles.

nanoparticles and this was more common for relatively larger particles. During spraying and atomization of the liquid some droplets may have been larger than the others and it is the particles formed from these droplets that may have shrunken due to solvent evaporation during the drying process. In general, the particle size distribution of the nanoparticles from both formulations was highly reproducible. Additionally, the nanoparticles were characterized for surface charge by measuring the Zeta potential, which is dependent on the formulation and processing conditions, such as amount of drug or surfactant accumulating on the surface during the particle formation. Surface charge is an important factor in predicting the interactions between the particles themselves and in determining their absorption characteristics following oral administration. While the two formulations had similar thermal properties and particle size and morphology, they had a significantly different zeta potential. Formulation A, which contained 29% amifostine, showed cationic charge (+2.8 mV), whereas formulation B, which contained 50% amifostine, showed anionic charge (−13.8 mV) (Table 1). This difference in zeta potential may be due to the difference in amifostine content. Since a cationic surface charge enhances particle absorption through gastrointestinal mucosa (El-Shabouri 2002), we selected formulation A for our further in-vivo study.

Tissue distribution

The results of the tissue distribution study in mice are shown in Table 3. A significant amount of the metabolic WR-1065 was detected in plasma as early as 30 min post-administration. On the other hand, no WR-1065 was detected in the plasma at 4 h. Like plasma, the brain, spleen and muscle also showed no WR-1065 at 4 h samples. The concentration of WR-1065 found in the brain

was $7.04 \mu\text{g g}^{-1}$ of tissue at 30 min and the concentration of WR-1065 in these samples at 2 h was below the detection limit. The fact that WR-1065 was detected in significant amounts in all tissues analysed at 30 min clearly demonstrates the effectiveness of orally administered nanoparticles to deliver the active metabolite in key target tissues. It is also clear from the data that there is some degree of selectivity in WR-1065 distribution. For example, in the gastrointestinal tract, jejunum had the highest concentrations followed by the stomach, while duodenum and ileum had the lowest concentrations. This selectivity may be related to the absorption behaviour of these tissues based on the size and charge of the particles. Histological studies are planned to confirm this possibility. The presence of significant amounts of WR-1065 in the bone marrow and kidney is of special interest because protection of these tissues from radiation damage is key to host survival and recovery.

Conclusions

The spray drying procedure produced amifostine nanoparticles with suitable properties for oral absorption. While the drug loading did not affect particle size and morphology, it did produce opposite surface charges. The data clearly demonstrate that amifostine nanoparticles given orally do deliver the drug in significant concentrations to a variety of tissues including key target tissues. It is also clear that there is some degree of selectivity in WR-1065 distribution in various tissues. This selectivity may be related to the differences in the absorptive capacities of various tissues for the nanoparticles. Histological studies are planned to confirm this hypothesis and we are currently evaluating this formulation for radioprotection efficacy in mice. In summary, this work demonstrates the feasibility of developing an orally effective formulation of amifostine that can be used clinically.

Table 3 Concentration of WR-1065 in plasma and various tissue samples collected up to 4 h following oral administration of amifostine nanoparticles

Tissue	Concn of WR-1065 ($\mu\text{g mL}^{-1}$ for plasma; $\mu\text{g g}^{-1}$ for all other tissue samples)			
	30 min	1 h	2 h	4 h
Plasma	309 (54)	211 (1.0)	186 (7)	ND ^a
Liver	260 (48)	116 (12)	109 (1.0)	102 (13.2)
Kidney	292 (52)	68 (16)	181 (55)	2.86 (0.86)
Stomach	19 (6)	40 (15.6)	82 (26)	68 (33.5)
Duodenum	2 (0.05)	2.7 (0.1)	35 (3.5)	13 (2.3)
Jejunum	115 (9)	128 (59)	143 (22)	78 (0.57)
Ileum	2.6 (0.5)	1.1 (0.3)	39 (3.5)	37 (16.7)
Bone marrow	60 (4)	36 (8)	15 (5)	21 (7.5)
Brain	7.04 (0.9)	0.3 (0.1)	ND	ND
Heart	65 (17)	26 (8)	65 (14)	ND
Spleen	37 (0.4)	26 (5)	19 (6)	6 (5)
Muscle	40 (10)	26 (9)	40 (11)	ND

Data are presented as the mean (s.e.m.). ^aNot detected.

References

- Alpar, H. O., Field, W. N., Hyde, R., Lewis, D. A. (1989) The transport of microspheres from the gastro-intestinal tract to inflammatory air pouches in the rat. *J. Pharm. Pharmacol.* **41**: 194–196
- Anne, P. R., Curran, W. J. (2002) A phase II trial of subcutaneous amifostine and radiation therapy in patients with head and neck cancer. *Semin. Radiat. Oncol.* **12**: 18–19
- Bockmann, J., Lahl, H., Eckert, T., Unterhalt, B. (2000) Blood titanium levels before and after oral administration of titanium dioxide. *Pharmazie* **55**: 140–143
- Bonner, H. S., Shaw, L. M. (2002) New dosing regimens for amifostine: a pilot study to compare the relative bioavailability of oral and subcutaneous administration with intravenous infusion. *J. Clin. Pharmacol.* **42**: 166–174
- Cassatt, D. R., Fazembaker, C. A., Bachy, C. M., Hanson, M. S. (2002) Preclinical modeling of improved amifostine (ethylol) use in radiation therapy. *Semin. Radiat. Oncol.* **12**: 97–102
- De Jaeghere, F., Allemann, E., Kubel, F., Galli, B., Cozens, R., Doelker, E., Gurny, R. (2000) Oral bioavailability of a poorly water soluble HIV-1 protease inhibitor incorporated into pH-sensitive particles: effect of the particle size and nutritional state. *J. Control. Release* **68**: 291–298
- Desai, M. P., Labhasetwar, V., Amidon, G. L., Levy, R. J. (1996) Gastrointestinal uptake of biodegradable microparticles: effect of particle size. *Pharm. Res.* **13**: 1838–1845
- Ebel, J. P. (1990) A method for quantifying particle absorption from the small intestine of the mouse. *Pharm. Res.* **7**: 848–851
- Eldridge, J. H., Hammond, C. J., Meulbroek, J. A., Staas, J. K., Gilley, R. M., Rice, T. R. (1990) Controlled vaccine release in the gut-associated lymphoid tissues. I. Orally administered biodegradable microspheres target the Peyer's patches. *J. Control. Release* **11**: 205–214
- El-Shabouri, M. H. (2002) Positively charged nanoparticles for improving the oral bioavailability of cyclosporine-A. *Int. J. Pharm.* **249**: 101–108
- Fatome, M., Courteille, F., Laval, J. D., Roman, V. (1987) Radioprotective activity of ethylcellulose microspheres containing WR 2721, after oral administration. *Int. J. Radiat. Biol. Relat. Stud. Phys. Chem. Med.* **52**: 21–29
- Feng, S. S., Huang, G. F. (2001) Effects of phospholipids as emulsifiers on controlled release of paclitaxel from nanoparticles of biodegradable polymers. *J. Control. Release* **71**: 53–69
- Florence, A. T. (1997) The oral absorption of micro- and nanoparticulates: neither exceptional nor unusual. *Pharm. Res.* **14**: 259–266
- Florence, A. T., Jani, P. U. (1993) Particulate delivery: the challenge of the oral route. In: Rolland, A. (ed.) *Pharmaceutical particulate carriers: therapeutic applications*. Marcel Dekker, New York, p. 82
- Godette, K. D. (2001) Clarification on the potential of subcutaneous ethylol as a radioprotective agent. *J. Clin. Oncol.* **19**: 1582–1585
- Guterres, S. S., Fessi, H., Barratt, G., Puisieux, F., Devissauquet, J. (1995) Poly(D,L-Lactide) nanocapsules containing non-steroidal anti-inflammatory drugs: gastrointestinal tolerance following intravenous and oral administration. *Pharm. Res.* **12**: 1545–1547
- Hussain, N., Jaitley, V., Florence, A. T. (2001) Recent advances in the understanding of uptake of microparticulates across the gastrointestinal lymphatics. *Adv. Drug Dev. Rev.* **50**: 107–142
- Jani, P. U., Halbert, G. W., Langridge, J., Florence, A. T. (1989) The uptake & translocation of latex nanospheres and microspheres after oral administration to rats. *J. Pharm. Pharmacol.* **41**: 809–812
- Jani, P., Halbert, G. W., Landridge, J., Florence, A. T. (1990) Nanoparticle uptake by the rat gastrointestinal mucosa: quantitation and particle size dependency. *J. Pharm. Pharmacol.* **42**: 821–826
- Jani, P. U., Florence, A. T., McCarthy, D. E. (1992) Further histological evidence of the gastrointestinal absorption of polystyrene nanospheres in the rat. *Int. J. Pharm.* **84**: 245–252
- Jenkins, P. G., Howard, K. A., Blackhall, N. W., Thomas, N. W., Davis, S. S., O'Hagan, D. T. (1994) Microparticle absorption from the rat intestine. *J. Control. Release* **29**: 339–350
- Koukourakis, M. I., Romanidis, K., Froudarakis, M., Kyrgias, G., Koukourakis, G. V., Retalis, G., Bahlitzanakis, N. (2002) Concurrent administration of docetaxel and stealth liposomal doxorubicin with radiotherapy in non-small cell lung cancer: excellent tolerance using subcutaneous amifostine for cytoprotection. *Br. J. Cancer* **87**: 385–392
- Lamperti, A., Ziskin, M. C., Bergey, E., Gorlowski, J., Sodicoff, M. (1990) Transdermal absorption of radioprotectors in the rat using permeation-enhancing vehicles. *Radiat. Res.* **124**: 194–200
- LeFevre, M. E., Olivo, R., Vanderhoff, J. W., Joel, D. D. (1978) Accumulation of latex in Peyer's patches and its subsequent appearance in villi and mesenteric lymph nodes. *Proc. Soc. Exp. Biol. Med.* **159**: 298–302
- LeFevre, M. E., Hancock, D. C., Joel, D. D. (1980) Intestinal barrier to large particulates in mice. *J. Toxicol. Environ. Health* **6**: 691–704
- Mu, L., Feng, S. S. (2001) Fabrication, characterization and in vitro release of paclitaxel loaded poly (lactic-co-glycolic acid) (PLGA) nanospheres prepared by the spray dry technique with phospholipids/cholesterol as additives. *J. Control. Release* **76**: 239–254
- Pamujula, S., Graves, R., Kishore, V., Mandal, T. K. (2004) Preparation and *in vitro* characterization of amifostine biodegradable microcapsules. *Eur. J. Pharm. Biopharm.* **57**: 213–218
- Payne, J. M., Sansom, B. F., Garner, R. J., Thomson, A. R., Miles, B. J. (1960) Uptake of small resin particles (1–5 microns diameter) by the alimentary canal of the calf. *Nature* **188**: 586
- Powel, J. J., Harvey, R. R., Ashwood, P., Wolstencroft, R., Gershwin, M. E., Thompson, R. P. (2000) Immune potentiation of ultrafine dietary particles in normal subjects and patients with inflammatory bowel disease. *J. Autoimmun.* **14**: 99–105
- Sanders, E., Ashworth, C. T. (1961) A study of particulate intestinal absorption and hepatocellular uptake: use of polystyrene latex particles. *Exp. Cell. Res.* **22**: 137
- Schuchter, L. M., Hensley, M. L., Meropol, N. J., Winer, E. P. (2002) Update of recommendations for the use of chemotherapy and radiotherapy protectants: clinical practice guidelines of the American Society of Clinical Oncology. *J. Clin. Oncol.* **20**: 2895–2903
- Srinivasan, V., Pendergrass, J. A., Kumar, K. S., Landauer, M. R., Seed, T. M. (2002) Radioprotection, pharmacokinetic and behavioural studies in mouse implanted with biodegradable drug (amifostine) pellets. *Int. J. Radiat. Biol.* **78**: 535–543
- Wang, F. J., Wang, C. H. (2003) Etanidazole-loaded microspheres fabricated by spray-drying different poly(lactide/glycolide) polymers: effects on microspheres properties. *J. Biomater. Sci. Polymer Edn.* **14**: 157–183